A novel Raman spectrum detection system based on an integrated optical biosensor

Li, Yang, Zhao, Haolan, Baets, Roel, He, Jian-Jun

SPIE.

A novel Raman spectrum detection system based on an integrated optical biosensor

Yang Li[ab], Haolan Zhao[b], Roel Baets[b], Jian-Jun He*[a]

[a]State Key Laboratory of Modern Optical Instrumentation, College of Optical Science and Engineering, Zhejiang University, Hangzhou 310007, China; [b]Photonics Research Group of Ghent University - IMEC And Center of Nano- and Biophotonics (NB-Photonics) of Ghent University, Ghent 9000, Belgium

ABSTRACT

In recent years, there has been a growing demand for hand held and miniaturized spectroscopic Raman systems that can be employed in the field to distinguish and quantify different analytes. In this paper, a novel and integrable system to detect a Raman spectrum is presented. We present the system principle, sensor design, experimental set-up and primary measurement results. In a conventional Raman setup, the four important components are: a light source, sensor, spectrometer and detector. We utilize a tunable laser as light source in the new Raman detecting system to replace the spectrometer by scanning the pump wavelength. A Raman sensor based on silicon nitride platform which has small size and high signal-background ratio is demonstrated in this paper to enable the excitation and the collection of the Raman signal using a plasmonic slot waveguide structure. Besides the tunable laser and the Raman sensor, there are two basic devices in our system, a narrow band-pass filter and a power detector. In this work, the Raman signal of the measured molecule 4-nitrothiophenol (NTP) is obtained by scanning the pump wavelength from 735 nm to 786 nm. The light source and detector in our experiment are implemented by discrete components. Silicon photonics promises the integration of a complete on-chip Raman spectroscope where the tunable laser, detector, sensor and filter can be integrated in a millimeter sized chip. We analyze the primary results measured by the discrete devices and discuss the feasibility of the on-chip integration in the end.

Keywords: Optical sensors, Raman spectroscopy, integrated optics, plasmonic waveguide

1. INTRODUCTION

Raman scattering is an inelastic scattering process. When incident photons are scattered by molecules, there is a net exchange of energy between the incident photons and the molecules. The photons lose a part of energy which is absorbed by the molecules to excite new vibrational states. The lost energy results in shifts in the frequency of the scattered photons compared to the frequency of the incident photons[1-3]. The amount of shifted frequency corresponds to vibrational modes of the molecules. Hence, Raman spectroscopy has the capability of identifying the molecules and quantifying their density [4-7]. It has been widely used as a mainstream analytic tool for analytic chemistry and biology. The major drawback of Raman spectroscopy is the extremely small cross-section of the spontaneous Raman scattering process. The inherent weakness of Raman signals necessitate advanced techniques and expensive devices with high performance to enhance and detect the signal. Conventional Raman setups are always bulky andexpensive. This makes it impractical for their widespread applications outside of the specialized labs.

More recently, with the development of integrated laser diodes, the applications of photonic integrated components have explosively grown, from telecom communications to biochemical sensing. The efforts of photonics integration have led to the advent of nanophotonic waveguides as a promising platform to enhance the spontaneous Raman signal. The advantages for utilizing a photonic chip to produce the Raman signal are:

1. Enhancement of spontaneous Raman scattering signal resulting from the effect of waveguide mode confinement.

2. Possibility of on-chip sensing system designs which consist of laser source, Raman sensor, filter, splitter, etc.

3. Reduction of the cost by the use of CMOS-compatible processes of mass fabrication of a device.

4. Reduction of the system size to micro-nano scale.

Recently on-chip Raman sensing systems based on the photonic integration have attracted the attention of many researchers. The waveguide mode is used to excite and/or collect the Raman signals in the sensor chips. High index contrast waveguides confine the light in a very small area, which leads to the enhancement of the field intensity and the improvement of the light-matter interaction efficiency[8,9]. Spontaneous Raman spectroscopy on photonic waveguides has been demonstrated to detect bulk liquid of isopropyl alcohol[10], biological monolayers[11] and toluene liquid[12,13]. The combination of a plasmonic structure and a dielectric waveguide has been proposed to further enhance the Raman signal intensity[14-18]. Nano-plasmonic antennas, microspheres and layers are able to confine the optical field in a tinier volume compared to dielectric waveguides[19-22].

Here we propose a new and integrable Raman sensing system where the Raman spectrum is obtained by utilizing a tunable laser to scan the pump wavelength. In this way, the spectrometer that plays an essential role in a conventional Raman detection set-up can be removed from the system. We previously reported an experimental configuration of plasmonic slot waveguides for monolayer sensing, where the Raman signal was excited from free-space and collected by the waveguide[23]. In that case, a noticeable and reproducible improvement of the signal-to-background ratio (SBR), which is the bottleneck in most on-chip Raman demonstrations[24,25], can be implemented. This paves the way for achieving a more compact on-chip Raman detection system consisting of laser source, Raman sensor, filter, splitter etc. The primary signal of the Raman spectrum was obtained by applying the Raman sensor in the novel detection system we proposed in this paper.

2. PRICIPLE OF THE SYSTEM

The flow charts in Fig. 1 introduce the fundamental components and the schematic of a conventional Raman spectroscopy system and the new system we proposed, respectively. A conventional detection set-up for Raman spectra is always composed of four essential parts as shown in the upper flow chart. The pump light with a fixed wavelength is provided by a continuous wave (CW) laser. The CW laser illuminates the Raman sensor, which contains the analytes. The Raman sensor may enhance the intensity of the signal by making use of some advanced technologies, such as surface enhanced Raman scattering, stimulated Raman scattering, etc. The Raman signals induced from the Raman sensor consist of spectrally distributed light. Therefore, a spectrometer plays a crucial role in a conventional Raman set-up. Finally, the power detector or detector array converts the optical signals into electrical signals. The sensitivity and resolution of the Raman set-up largely depend on the performance of spectrometer. However, a spectrometer of high quality is expensive and takes up most space of the Raman system. In the area of photonic integration, the structure of an on-chip spectrometer is also relatively large and complex.

Conventional system:

CW laser → Raman sensor → Spectrometer → Power detector

System in this paper:

Tunable laser → Raman sensor → Bandpass filter Center wavelength = λ_d → Power detector
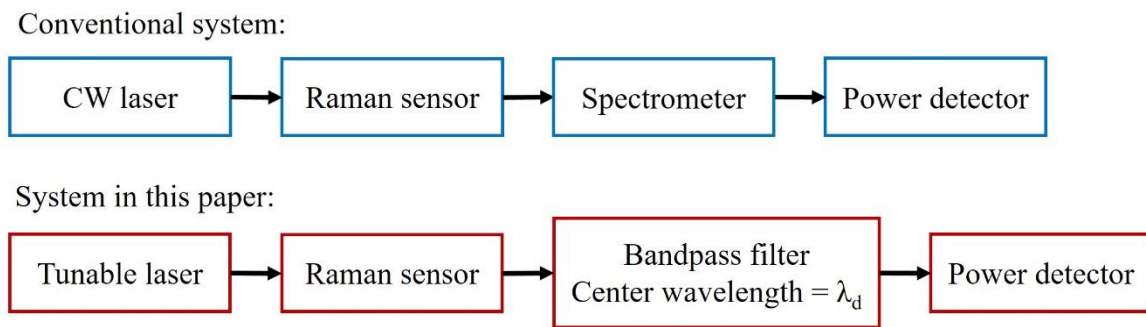
Figure 1. Flow diagrams of the conventional Raman detection system and the novel Raman detection system.

The integrable tunable semiconductor laser has achieved considerable development in recent years. It is widely applied in both industry and research labs. The lower flow chart in Fig. 1 illustrates the design of our Raman detection system, where we utilize a tunable laser as the light source and replace the spectrometer with a band-pass filter. Before we introduce the working principle of this system, we elaborate a unique characteristic of Raman scattering due to which this system is practicable in the detection of Raman spectrum. The wavelength shifts between the pump light and the Stokes peaks are constant for different pump wavelengths. They only depend on the vibrational modes of the analyte molecules. Supposing the molecules are excited by light with wavelength λ_{p1} and wavelength λ_{p2} respectively and $\lambda_{p2} = \lambda_{p1} + \Delta\lambda$, the Raman spectra are shown in Fig. 2. The green spectrum is obtained by pump light of λ_{p1} and the red spectrum is obtained by pump

light of λ_{p2}. Since the Raman shifts are independent of pump wavelength, these two spectra have identical outline and Raman peak information.
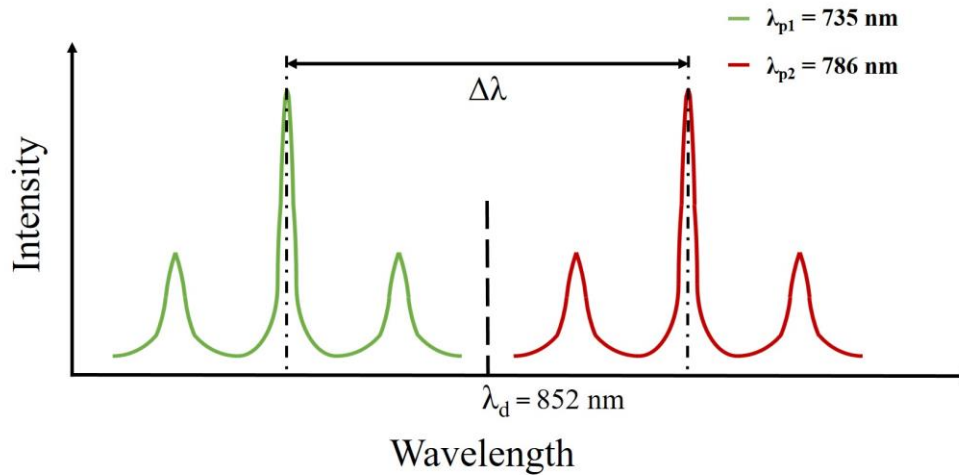
Figure 2. The Raman spectra with pump wavelengths of λ_{p1} nm and λ_{p2} produced by identical molecules.

In our new system, the tunable laser is used to illuminate the Raman sensor and scan the pump wavelength. In the case of Fig. 2, the Raman spectrum produced by Raman sensor moves from green one to red one when the pump wavelength is swept from λ_{p1} to λ_{p2}. The value of λ_d is between the right end of green spectrum and the left end of red one. During this process, the complete green spectrum will pass through the dashed line at λ_d only if the width of the scanning range $\Delta\lambda$ is larger than the width of the Raman spectrum. Hence the intensity of light with wavelength λ_d changes with the fluctuation of the spectral profile. We place a narrow-band-pass filter with center wavelength at λ_d before the power detector in our Raman system. The optical power passing through the filter changes as the pump scanning runs. The Raman spectral information of the analyte is reflected through the relationship between the optical power on detector and the pump wavelength. So this Raman detection system is capable of extracting the information of the Raman spectrum, especially the Raman peaks of the analytes, without the use of a spectrometer. It is a promising solution for an all-on-a-chip Raman sensing system. The removal of spectrometer alleviates the burden of integration, leading to a more compact and miniaturized photonic functional chip.

In this paper, we demonstrate this system with a silicon nitride plasmonic slot waveguide[23] as the Raman sensor. The pump laser illuminates the plasmonic slot waveguide obliquely from free space. The Raman sensor is functionalized with a monolayer of 4-nitrothiophenol (NTP) molecules. The pump wavelength in the experiment is scanned from 735 nm (λ_{p1}) to 786 nm (λ_{p2}), which means $\Delta\lambda$ is 51 nm. An ultra-narrow band-pass filter with the central transmitting wavelength of 852 nm is chosen to play the role of the dashed line in Fig. 2. Ideally only the light of 852 nm (λ_d) is able to be received by the detector in our demonstration. Here the values of λ_{p1}, λ_{p2} and λ_d are assigned based on the performances of the Raman sensor as well as the properties of the analytes (NTP). The characteristics of the Raman sensor and the properties of the analytes will be introduced in the next section.

3. CHARACTERISTICS OF THE SINGLE RAMAN SENSOR

The Raman sensor's capability to excite and collect Raman signals is essential to the performance of the whole system. We chose a silicon nitride plasmonic slot waveguide[23] as the Raman sensor. An NTP monolayer was labeled on the surface of the gold-coated slot waveguide. The physical theory, design layout, and experimental configuration of the Raman sensor[23] had been reported before, hence were omitted in this paper. Before applying this Raman sensor in the system, it is indispensable to examine its properties as well as the Raman activity of NTP molecules.

To test the properties of the Raman sensor, a pump laser of 785 nm was used to excite the Raman scattering of NTP. The power of pump light was 2.5 mW. The Raman spectrum of the NTP molecules produced by the Raman sensor was illustrated in Fig. 3 (a). The characteristic Raman peaks of 1100 cm^{-1}, 1340 cm^{-1} and 1560 cm^{-1} with high intensity and

signal-background ratio were clearly detected. The blue spectrum was actual data recorded by spectrometer and the yellow dashed spectrum was processed result after polynomial smoothing. The integration time of the spectrometer in the test was 20 seconds, during which the Raman sensor had excellent performance. However, when applied in our new system, the Raman sensor had to be exposed to the irradiation of the pump light for much longer time to complete the scanning of the pump wavelength. Hence, besides the signal intensity and signal-background ratio, the signal stability under long-time continuous illumination is required in our new detection system.
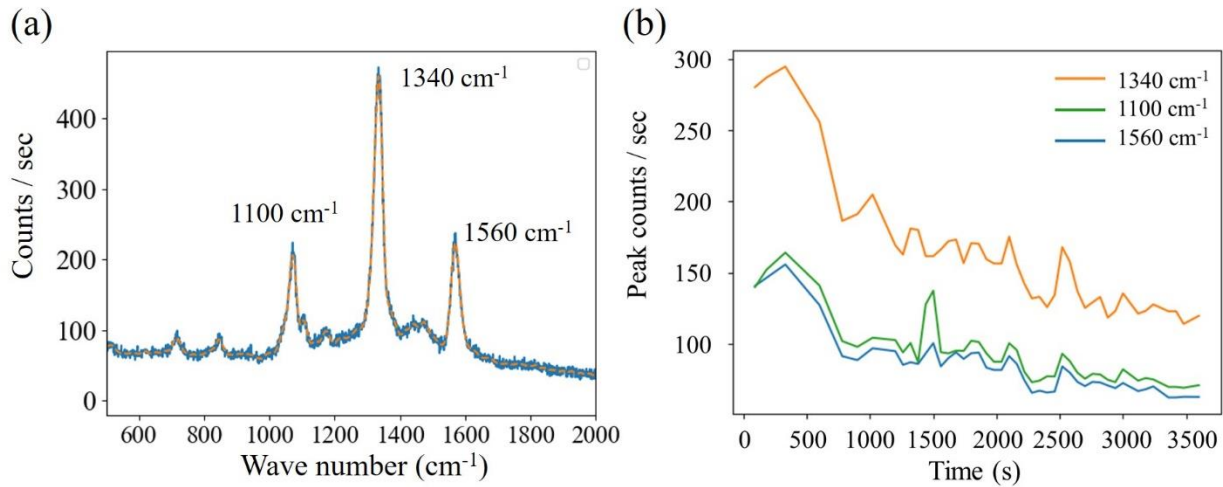
Figure 3. (a) The Raman spectra measured with CW laser light of 785 nm. (b) The count values of the Stokes peaks recorded under one-hour illumination.

To test the stability of the signal, we illuminated the Raman sensor continuously for one hour with pump light of 785 nm. The incident power was 2.5 mW. The Raman spectra were recorded every 5 mins. We extract the peak count values of 1100 cm^{-1}, 1340 cm^{-1} and 1560 cm^{-1} from all spectra and plot their changes over time in Fig. 3(b). In the first ten minutes, the signals decay fast. This may be caused by the photothermal effect[26] of the gold layer in the plasmonic slot waveguide. The gold layer absorbed the photons rapidly and released them as heat in the first ten minutes. This heat could affect the activity of the analytes. Although the signals decay fast in the first ten minutes in Fig. 3(b), they later remain relatively stable. This indicates the Raman sensor can satisfy the basic requirements of the signal strength and stability for our system after the first ten minutes.
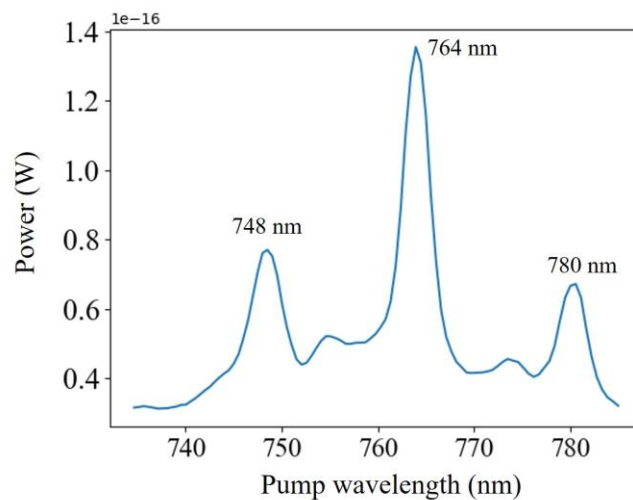
Figure 4. The estimated power of the light transmitting through the narrow band-pass filter at different pump wavelengths.

Supposing the wavelength shifts between characteristic peaks and pump light were constant for any pump wavelengths, the Raman spectra excited by other pump wavelengths to be scanned were deduced. In our system set-up, only the light transmitting the narrow-band filter with transmission wavelength of 852 nm can be received by power detector. According to the deduced spectra, we estimated the optical power transmitted through the filter over different pump wavelengths in Fig. 4. Here the left peak at 748 nm corresponds to the Raman peak at 1560 cm^{-1}, the peak at 764 nm corresponds to the Raman peak at 1340 cm^{-1}, and the peak at 780 nm corresponds to the Raman peak at 1100 cm^{-1}. In the estimation, the transmission spectrum of narrow-band filter is modeled as a rectangular window of which the width is 4 nm, the center wavelength is 852 nm and the transmission coefficient is 0.98.

4. SYSTEM SET-UP AND PRIMARY RESULTS

We tested the system with discrete devices. Fig.5 illustrats the diagram of experimental set-up. The Ti: Sapphire laser was used to scan the pump wavelength from 735 nm to 786 nm. The pump light was collimated into free space through a fiber collimator. A polarizer was installed to ensure TE polarization of the pump. There was background light in the wavelength range of 800 nm - 850 nm caused by nonlinear effects in the laser, no matter what the pump wavelength was. This would interfere with the detection of the Raman peaks whose wavelengths were in the range of 800 nm - 850 nm. We placed a short-pass filter to clean the pump laser by suppressing the light with the wavelength longer than 800 nm. The cleaned pump beam was focused onto the Raman sensor by an objective (Nikon, 50X, NA=0.6). Fiber collimator, polarizer, short-pass filter and objective were mounted on a plate with adjustable angle. The incident angle in the experiment was 75°. The induced Stokes lights and a fraction of pump light were collected by another objective which focused on the output facet of the sample. The long-pass filter was used to reject the pump light. The central wavelength of the narrow-band filter (Semrock LL01-852-12.5) was 852 nm. We utilized a cooled camera (Andor iDus 416 deep-cooled CCD camera) to detect the optical power transmitted through the filter.
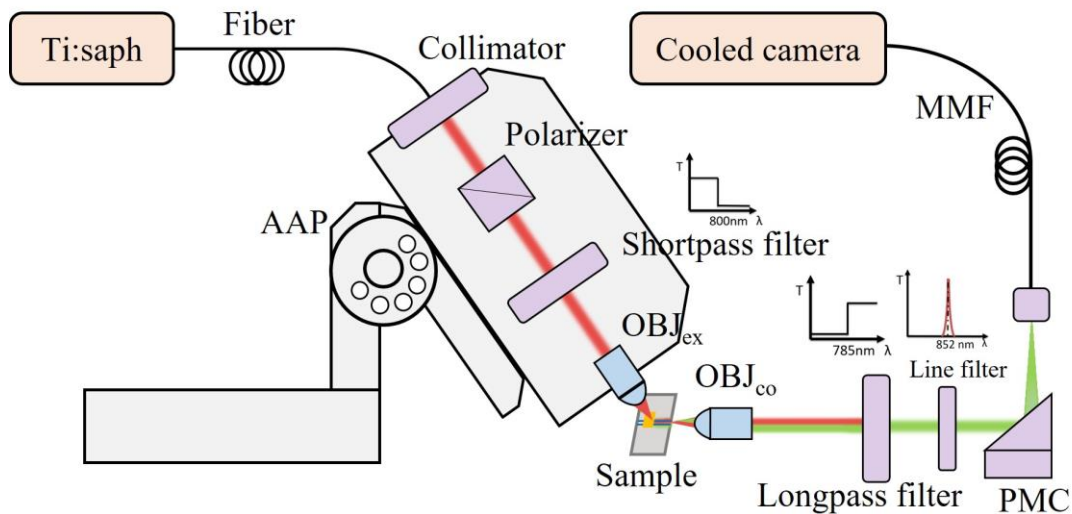
Figure 5. The schematic diagram of the free-space excitation experimental setup. Ti:saph: tunable Ti:sapphire laser, OBJex: objective (50×, NA=0.6) for free-space excitation, AAP: adjustable angle plate, OBJco: objective (50×, NA=0.65) for signal collection, PMC: parabolic mirror collimator, MMF: multimode fiber.

We scanned the pump with an interval of 0.5 nm. It took 40 minutes to complete the sweep of the pump wavelength. The results are plotted in Fig. 6. The blue spectrum shows experimental results. To compare the measurement to the estimation, the estimated result (dashed curve) is also shown in Fig. 6. We clearly observed the emergence of three peaks. The position and the height of the peaks in the experimental results roughly agreed with the estimation. There were slight and acceptable deviations of the characteristic peak intensity. These deviations were caused by the fluctuations in sensor performance.
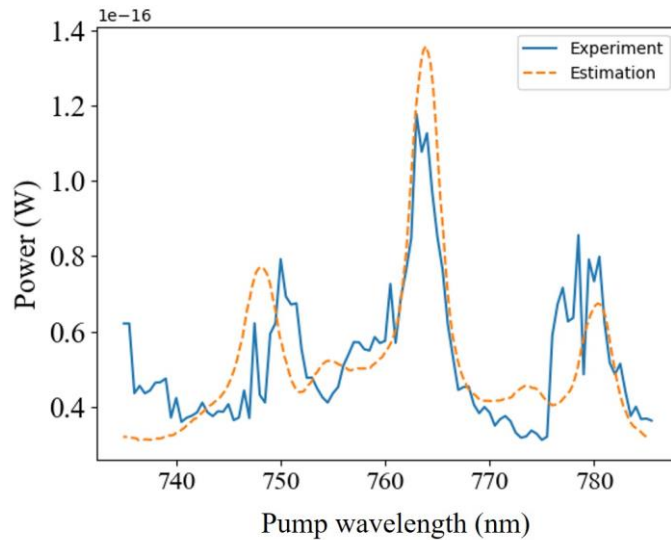
Figure 6. The signal power obtained through the cooled camera. The blue spectrum is the experimental result and the dashed spectrum is the estimated result.

5. CONCLUSION

We reported a new Raman detecting system in this paper including the principle, design, set-up and measurement results. The Raman sensor, most essential component of the system, was tested individually with a fixed pump wavelength of 785 nm. The Raman signal intensity and the stability of the sensor were analyzed. We utilized a tunable laser as the light source and a narrow bandpass filter in the new Raman detecting system to replace the spectrometer by scanning the pump wavelength. In this system, only one high-quality detector is required rather than an array or a camera. We implemented this system with discrete components as a proof-of-concept demonstration. The information of characteristic Raman peaks was contained in the relation between the optical power and pump wavelength. The Raman signal of NTP was obtained by scanning the pump wavelength from 735 nm to 786 nm. This indicated the system was efficient and feasible. It is possible to implement the system design into on-chip photonic integrated circuit. The difficulty of integration and the size of on-chip system are reduced because the system excludes the spectrometer. Our system is time sequential and therefore the measurement will typically take longer than a conventional spectrometer-based system, which works in parallel. This is a disadvantage for broad spectra. However, the system is practical if only a relatively narrow part of a Raman spectrum needs to be measured in a given application.

ACKNOWLEDGMENT

REFERENCES

[1] D.A. Long, The Raman Effect: A Unified Treatment of the Theory of Raman Scattering by Molecules, John Wiley & Sons Ltd. West Sussex, 351-354 (2002).
[2] J.R. Ferraro, Introductory Raman spectroscopy, Academic press, (2003).
[3] J. J. Laserna, Modern Techniques in Raman Spectroscopy, John Wiley & Sons, (1996).

[4] J. X. Cheng and X. S. Xie, Coherent Raman Scattering Microscopy, Taylor & Francis, (2012).

[5] C. Krafft, G. Steiner, C. Beleites, and R. Salzer, "Disease recognition by infrared and Raman spectroscopy." J. Biophotonics, vol. 2(1-2), 13-28, (2009).

[6] M.-L. Xu, Y. Gao, X. X. Han, and B. Zhao, J. Agric. "Detection of Pesticide Residues in Food Using Surface-Enhanced Raman Spectroscopy: A Review" Food Chem. Vol. 65, 6719-6726, (2017).

[7] B. Bao, J. Riordon, F. Mostowfi, and D. Sinton, "Microfluidic and nanofluidic phase behaviour characterization for industrial CO2, oil and gas." Lab Chip, vol. 17, 2740-2759, (2017).

[8] J.S. Kanger, C. Otto, M. Slotboom and J. Greve, "Waveguide Raman spectroscopy of thin polymer layers and monolayers of biomolecules using high refractive index waveguides." J. Phys. Chem, vol. 100(8), 3288-3292, (1996).

[9] J.F. Rabolt, R. Santo and J.D. Swalen, "Raman measurements on thin polymer films and organic monolayers." Appl. Spectrosc, vol. 34(5), 517-521, (1980).

[10] W. Xie, B. Walkenfort, S. Schlücker, "Label-free SERS monitoring of chemical reactions catalyzed by small gold nanoparticles using 3D plasmonic superstructures." J AM CHEM SOC, vol. 135(5), 1657-1660, (2012).

[11] X. M. Qian, S. M. Nie, "Single-molecule and single-nanoparticle SERS: from fundamental mechanisms to biomedical applications." CHEM SOC REV, vol. 37(5), 912-920, (2008).

[12] Zilong Wang, Michalis N. Zervas, Philip N. Bartlett, and James S. Wilkinson, "Surface and waveguide collection of Raman emission in waveguide-enhanced Raman spectroscopy," Opt. Lett, vol. 41(17), 4146-4149, (2016).

[13] Zilong Wang, Stuart J. Pearce, Yung-Chun Lin, Michalis N. Zervas, Philip N. Bartlett, and James S. Wilkinson, "Power Budget Analysis for Waveguide-Enhanced Raman Spectroscopy," Appl. Spectrosc, vol. 70(8), 1384-1391, (2016).

[14] X. Hong, D. Wang, Y. Li, "Kinked gold nanowires and their SPR/SERS properties." CHEM COMMUN, vol. 47(35), 9909-9911, (2011).

[15] G. Das, F. Mecarini, F. Gentile, F. D. Angelis, HG. M. Kumar, P. Candeloro, C. Liberale, G. Cuda, E. D. Fabrizio, "Nano-patterned SERS substrate: Application for protein analysis vs. temperature." Biosens.Bioelectron, vol. 24, 1693-1699, (2009).

[16] Y. Zhao, B. Chu, L. Zhang, F. Zhao, J. Yan, X. Li, Q. Liu, Y. Lu, "Constructing sensitive SERS substrate with a sandwich structure separated by single layer graphene." Sens. Actuators B Chem, vol. 263, 634-642, (2018).

[17] Y. Zhao, X. Li, M. Wang, L. Zhang, B. Chu, C. Yang, Y. Liu, D. Zhou, Y. Lu, "Constructing sub-10-nm gaps in graphene-metal hybrid system for advanced surface-enhanced Raman scattering detection." J ALLOY COMPD, vol. 720, 139-146, (2017).

[18] A. Dhakal, A. Z. Subramanian, P. Wuytens, F. Peyskens, N. L. Thomas, and R. Baets, "Evanescent excitation and collection of spontaneous Raman spectra using silicon nitride nanophotonic waveguides," Opt. Lett, vol. 39, 4025-4028, (2014).

[19] A. Dhakal, P. C. Wuytens, F. Peyskens, K. Jans, N. L. Thomas, and R.Baets, "Nanophotonic Waveguide Enhanced Raman Spectroscopy of Biological Submonolayers" ACS Photonics, vol. 3, 2141-2149 , (2016).

[20] Y.-F. Xiao, Y.-C. Liu, B.-B. Li, Y.-L. Chen, Y. Li, and Q. Gong, "Strongly enhanced light-matter interaction in a hybrid photonic-plasmonic resonator," Phys. Rev. A, vol. 85, 31805, (2012).

[21] P. Vasa and C. Lienau, "Strong light–matter interaction in quantum emitter/metal hybrid nanostructures," ACS Photonics, vol. 5, 2–23, (2018).

[22] J. A. Schuller, E. S. Barnard, W. Cai, Y. C. Jun, J. S. White, and M. L. Brongersma, "Plasmonics for extreme light concentration and manipulation," Nat. Mater, vol. 9, 193–204, (2010).

[23] Y. Li, H. Zhao, A. Raza, S. Clemmen and R. Baets, "Surface-Enhanced Raman Spectroscopy Based on Plasmonic Slot Waveguides With Free-Space Oblique Illumination," J Quantum Electron, vol. 56(1), 1-8, (2020).

[24] A. Dhakal, P. C. Wuytens, A. Raza, N. L. Thomas and R.Baets, "Silicon nitride background in nanophotonic waveguide enhanced raman spectroscopy." Materials, vol. 10(2), 140, (2017).

[25] N. L. Thomas, A. Dhakal, A. Raza, F. Peyskens, and R. Baets, "Impact of fundamental thermodynamic fluctuations on light propagating in photonic waveguides made of amorphous materials," Optica, vol. 5(4), 328-336, (2018).

[26] M. Rycenga, Z. Wang, E. Gordon, C. M. Cobley, Y. Xia, Probing the photothermal effect of gold-based nanocages with surface-enhanced Raman scattering (SERS). Angew Chem Int Ed Engl, vol. 48(52), 9924-9927, (2010).